Energy & Buildings 273 (2022) 112368

Contents lists available at ScienceDirect

Energy & Buildings

journal homepage: www.elsevier.com/locate/enb

A monthly performance comparison of green infrastructures enhancing urban outdoor thermal comfort

Luigi Schibuola, Chiara Tambani *

University IUAV of Venice, Dorsoduro 2206, 30123 Venice, Italy

A R T I C L E I N F O

Article history:
Received 11 May 2022
Revised 18 July 2022
Accepted 5 August 2022
Available online 11 August 2022

Keywords:
Urban microclimate
Local climate zones
Mitigation strategies
ENVI-met
PET monthly assessment

A B S T R A C T

Among the problems caused by the increase of the urban heat island phenomenon, the worsening of the outdoor thermal comfort at pedestrian level was addressed to improve urban resilience. Starting from the analysis of a real urban area in Venice, Italy, the study was extended to different urban forms classified by the Local Climate Zones (LCZs) method. The Physiological Equivalent Temperature (PET) calculated with the ENVI-met code was used to evaluate outdoor thermal comfort. Different mitigation strategies were compared for the whole summer period. For this purpose, a monthly assessment was performed using the monthly mean day approach rather than the usual single days analysis. A new index (%DPET) was proposed, indicating the percentage reduction in the discomfort rate in PET of the original scenario achieved by mitigation measures. The results show that the largest PETs, corresponding to very hot human thermal sensation, for the original scenario occur in the case of lowrise buildings. In this case, green and cool roofs provide their best performances and the seasonal %DPETs reach 9.1% and 7.5%, respectively. Green wall technology is the most effective in all urban forms studied with %DPET values ranging from 28% to 115%, sometimes reaching the neutral comfort level.

1. Introduction

Increasing urbanization and the next climate forecast promote urban heat island (UHI) effect problems and thus the challenge of ensuring adequate quality of life and health in urban areas [1,2]. Urban quality of life requires acceptable comfort conditions even outdoors, especially at pedestrian level. However, simply transferring comfort indices from indoor to outdoor environments has proven to be inadequate. This is due to the larger number of parameters involved in human thermal balance in the case of the outdoor environment. For this reason, indices developed specifically for the outdoors were adopted such as the Physiological Equivalent Temperature (PET) [3], the Outdoor Standard Effective Temperature (OUT_SET) [4] and the Universal Thermal Climate (UTCI) [5]. In particular, the PET index is the most widely used index nowadays [6] due to its ease of application and the possibility to be used in different climatic zones. For the European climate, a scale elaborated for Midwest Europe is usually used.

In terms of strategies to improve outdoor comfort, most studies have focused on the cooling effect of the green spaces on the ground level, such as parks and gardens, which reduce air and surface temperatures [7]. When greening measures on the ground are not feasible, efforts must be directed toward mitigation solutions applied to buildings. For this aim, three basic typologies can be considered [8]: cool or green surfaces on the roof and vertical greening on the façade.

The use of materials or coatings with a high albedo coefficient permits to reduce the surface temperature obtaining in this way the so-called cool surfaces [9]. Cool pavements can result from the application of flooring materials. Although many studies [10,11] have highlighted that this increase in reflectance in urban open spaces lowers the air temperature at pedestrian level, but it also penalizes thermal comfort due to a higher mean radiant temperature. For this reason, cool pavement technology was not considered in this work. As concerns cool roofs, several cool materials have been developed for this purpose, which are characterized by a high reflectivity for the visible or infrared quota of solar radiation [12,13]. These solutions have the general advantage of being easy to apply to existing roofs. One method to quantify the characteristics of a cool roof is to evaluate its Solar Reflectance Index (SRI) [14]. SRI is calculated based on solar reflectance and thermal emissivity values that also account for wind effects. This index is often used in green building rating procedures such as Leadership in Energy and Environmental Design (LEED) [15].

* Corresponding author.
E-mail address: chiara.tambani@iuav.it (C. Tambani).

https://doi.org/10.1016/j.enbuild.2022.112368
0378-7788/

Integrating vegetation into the building envelope is another strategy to mitigate thermal discomfort. In fact, greenery reduces solar heat gain [16,17] and evaporates water through evapotranspiration, a process that has a cooling effect on the environment. In this way, the surface temperature is lowered, and the emitted longwave radiation is reduced. Green roofs are divided into two main types: intensive and extensive green roofs. Intensive green roofs are roof gardens without restriction of available plants such as shrubs and trees [18]. They require deep soil substrates and are therefore very heavy, resulting in high costs for support structures and maintenance [19,20]. Extensive green roofs are characterized by vegetation that requires a thin soil substrate, obtaining in this way lightweight systems at low cost. Other diffuse characteristics include low maintenance and minimal or low irrigation [21]. For these reasons, extensive green-roofs are much more commonly used in practice than intensive green-roofs [22]. Green wall is a term that refers to the technology in which walls are covered with plants. In general, green walls can be divided into two broad categories, green facades and living walls. Green facades consist of plants growing on the building envelope. The plants can climb directly on the wall or use additional supports such as trellises [23]. The root of the climbing plant can be placed either in the ground or in soil positioned in modular panels on walls [24]. Living wall systems consist of pre-vegetated panels, attached vertically to the structural wall or to a frame.

On the other hand, an investigation on the effects of a mitigation technology cannot ignore the urban context in which it is applied. Therefore, the generalization of the results requires a precise classification of the urban contexts considered in the study. An urban classification can be based on the use of local climate zones (LCZ) [25]. The basic parameters that characterize each LCZ are the height and spacing of buildings, percentage of permeable surface, tree density, and soil moisture [26]. LCZs can be used in UHI modeling because they provide numerical data about urban canopy [27]. Seventeen LCZ types have been introduced, ten of which are related to urban canopy parameters and seven of which are related to land-cover types. Most methods for determining the appropriate LCZ in relation to an urban area are based on a procedure consisting in an automatic LCZ mapping proposed by [28], and adopted by the World Urban Database and Access Portal Tools (WUDAPT) project to produce consistent LCZ maps for entire cities [29].

In this paper, the possibility of reducing thermal discomfort at pedestrian level during summer months was investigated for different LCZs where greenery on the ground is often lacking and where greenery improvement is not possible. For this aim an urban area in the mainland of the city of Venice was selected. This area was extracted from WUDAPT's map of Europe and classified as LCZ 2 compact midrise. The study only considers mitigation technologies that can be applied to building envelopes. Special care was taken to evaluate the impact of the height of the buildings on their effectiveness. Therefore, only the height of the buildings was changed to create the models of the other two LCZs from the real one: a compact lowrise and a compact highrise. The study finally addressed these three LCZs. The analysis was based on the simulation of the urban microclimate using the ENVI-met software [30]. ENVI-met is a Computational Fluid Dynamics (CFD) software that has been widely used and tested [31,32] to evaluate the effects of various urban characteristics on microclimate including the presence of trees, density, types and dimensions of buildings, and various building materials [33–36]. The simulations were performed using the recent version V 4.45, released in summer 2020. ENVI-met is used to assess the impact of various outdoor environment improvement strategies in urban areas. This program includes the BioMet sub-module to calculate the PET index. The application of this software provided the PET indices for the studied area. As detailed in Section 4, this work aims to contribute to the knowledge of the benefits of greenery applied to buildings in terms of improving outdoor human comfort at the street level. An innovative monthly approach is applied to evaluate the performance of these mitigation strategies using the new features of ENVI-met 4.45 in a climate and urban forms still not investigated. To this end, a new index derived from PET is introduced.

2. Materials and methods

2.1. The investigated area

The mainland of Venice is the territory on the mainland coast of the Venice Lagoon. The rapid development, without a master plan, led to a certain disorder. The urban layout was deeply modified, with radical changes to city areas and the demolition of monuments and historic sites. From the last decade of the twentieth century, the expansionism was exhausted, and this area became the object of an urban renewal aimed at improving both its appearance and its quality of life. At this moment, the introduction of green spaces such as gardens has mainly interested the suburban neighborhoods, while interventions in the city center are still lacking, due to the difficulty of introducing green spaces and public gardens in the built center, where the classified areas refer to the compact zones. For this reason, this study is dedicated to the city center to evaluate the possibility of different measures to mitigate the urban heat island by applying solutions directly to the building envelope. Most of the city center is occupied by the three compact LCZs typologies: LCZ 1 compact highrise, LCZ 2 compact midrise and LCZ 3 compact lowrise [25]. In Venice urban mainland the predominant LCZ is compact midrise. For this reason, the focus for this study is on the compact midrise area reported in Fig. 1. Fig. 1b shows the part of the map extracted by WUDAPT, with the LCZ colors reported in Fig. 1a, which individuates the studied area (LCZ 2) from the surrounding area where only LCZs 2 and LCZs 5 are present. Fig. 1c is a picture of the analyzed area. The investigated area is a rectangle of 90x126 m (total area 11844 m^2).

In the studied area there are 20 buildings with a variable height between 20 and 40 m. The average ratio of height to width of the street canyons is 1.74. The percentage of the building footprint to the total footprint is 53 %, while the rest of the area is almost completely cemented and thus impervious (44 % of the total area). There are few trees and small permeable flowerbeds (3 %). The building volume density in relation to the total area is 7.08 m^3/m^2. The average height of buildings in the area is 18.4 m. Based on these values for urban geometry and surface cover parameters, the studied area can be classified as LCZ 2 compact midrise. To directly assess the impact of building heights, two additional compact LCZs were modeled by simply halving and doubling the building heights in the studied area to obtain an LCZ compact lowrise and an LCZ compact highrise, respectively, in this way.

2.2. The monitoring and meteorological data

A measurement of outdoor air temperature was made during the summer of 2019, i.e., between June and September. From these limited measurements, four days (June 22, July 15, August 18, and September 10) were selected to test the ENVI-met model of the area investigated as described in the Results section. A Hanwell data logger model ML4109 was used for the measurement. As regards measurement accuracy, the NTC temperature sensor has an accuracy of ±0.1 °C at 20 °C. The measurement was performed by installing the device in a location in the center of the studied area, in a courtyard, at a height of 1.80 m above the ground and shielded from solar radiation. The installation position is indicated by a blue dot in Fig. 1c. A preliminary simulation with ENVI-met

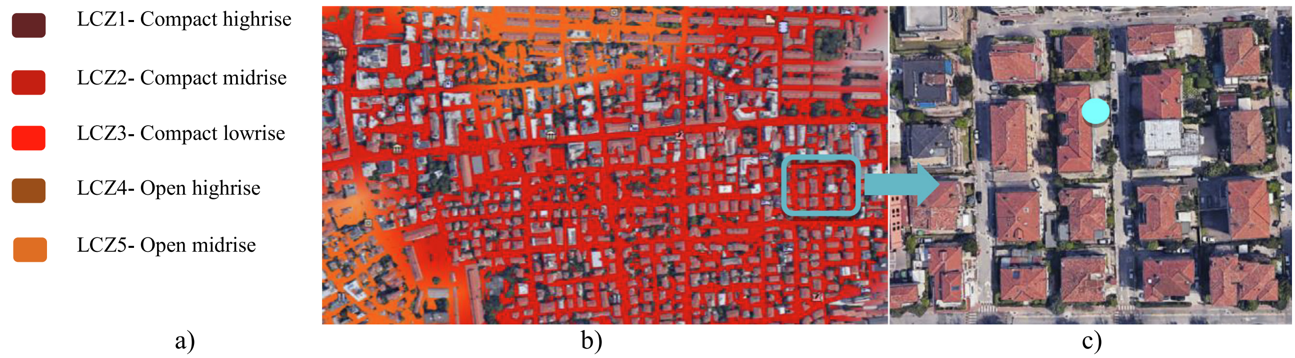

Fig. 1. LCZ colors (a) applied by WUDAPT to a part of the map of Venice b) and the analyzed area c).

was used to verify that this position was representative of the average thermal conditions in this urban area. Temperature was recorded every hour.

The weather conditions used to compare the performance of the different mitigation strategies through ENVI-met code simulations were instead based on actual weather data spanning the entire period from June to September 2019. These data were provided by the regional environmental agency ARPAV and collected by a meteorological station installed in the urban context and located near the analyzed area. The corresponding weather file is referred to here as the ARPAV weather file. The ARPAV weather data was used to create the corresponding EnergyPlus weather (EPW) file, according to [37]. However, due to the excessive computational time of ENVI-met, it was not possible to run complete simulations for all cases analyzed, which spanned the entire summer period, so a representative day was chosen for each month. This day is the monthly average built by the arithmetic means of outside temperature, radiation, relative humidity, and wind speed/direction at hourly time step. Peak and mild weather conditions are averaged in the monthly mean day to provide a mean condition. Unlike a single real day, the monthly mean day contains information about the frequency distribution of all the weather parameters throughout the month. The reference to a day that is representative of an entire month allows to reduce the computation time in hourly simulations of long-term periods. This is especially useful when sophisticated programs are used to perform demanding simulations. For this reason, it is often used in simplified performance evaluations of building systems. The same approach is now proposed to assess the seasonal performance of the mitigation solutions at the urban area scale. For this purpose, the full forcing procedure of the meteorological data was chosen in the simulations of ENVI-met, as foreseen by the program. This procedure uses these meteorological data directly in the simulation. Since precipitation was not available in our case, these data were not forced, an option allowed by the program allows. Since this analysis was dedicated to summer comfort conditions, the average values for September refer only to the period between the 1st and the 15th of the month, since the rest of this month is characterized by mild weather. The hourly data of the four monthly averages are shown in Fig. 2.

These four days were implemented in the ARPAV EPW file as replacements for the four original days and later used in the simulation with ENVI-met. In this paper they are mentioned only with the name of the corresponding month.

2.3. The ENVI-met code and the specific urban model of the case study

ENVI-met is a software that uses three-dimensional modeling to simulate the microclimate of the urban environment in the presence of surface-plant-air interactions at the microscale. It applies the k- ε turbulence model to solve the Reynolds averaged Navier-Stokes equations in a spatial grid at each time step [30]. The main input data required by ENVI-met are meteorological data, features and characteristics of ground surfaces, vegetation, and buildings [38]. The ability of ENVI-met to simulate urban thermal conditions under different weather conditions and in different countries was verified in several studies [39–42]. In [43] the daily profiles of outdoor air temperature from field measurements were compared with the corresponding values obtained by ENVI-met simulations. In this way, an excellent coefficient of determination R^2 of more than 0.8 was found. Similarly, [44] performed model validation in the case of a green roof simulation where air temperature was studied on two green roofs and one bare roof. They found a strong agreement between the simulations and the on-site measurements for both green roofs (R^2 equal to 0.95) and the bare roof (R^2 equal to 0.96).

For the digitization of the studied area (midrise case) in ENVI-met, a grid resolution of 2 × 2 × 2 m was used. In this way, the net investigated area of 126 × 94 m required a horizontal grid of 63 × 47 cells. Moreover, to ensure the stability of the simulation, 6 nested grids were used. As for the height, a total height of 60 m was used, i.e. 30 cells, which is higher than the minimum height required, which is twice that of the tallest building (24 m in our case) [45]. This height ratio was also maintained for highrise and lowrise simulations.

The digitized model in relation to the midrise case study introduced in ENVI-met is illustrated in Fig. 3, where an example of the graphical output of the program is shown in relation to a single time step (1 pm) of a daily simulation in August. In detail, the maps of outdoor air temperature at a height of 1.8 m are shown on the digitized surface (Fig. 3a). In the model, the albedo of the road pavement and of the cemented soil was assumed to be 0.2, and that of the traditional tile roof was assumed to be 0.3 [46]. As for the thermal transmittance of the building structures, the external walls have a U-value of 0.9 W/m^2 °C and the roofs 1.67 W/m^2°C, since they are usually not insulated in this urban area. These are typical thermal transmittances for Italian buildings structures [47].

2.4. The physiological equivalent temperature (PET) and the proposed PET indices

The PET index considers important variables of the outdoor environment in addition to thermohygrometric conditions, human metabolism, heat exchange and the parameters that influence it. PET is defined as the air temperature at which, in a reference indoor environment (without wind and solar radiation), the energy budget of the human body is balanced with the same core and skin temperature as in the outdoor condition to be evaluated. With

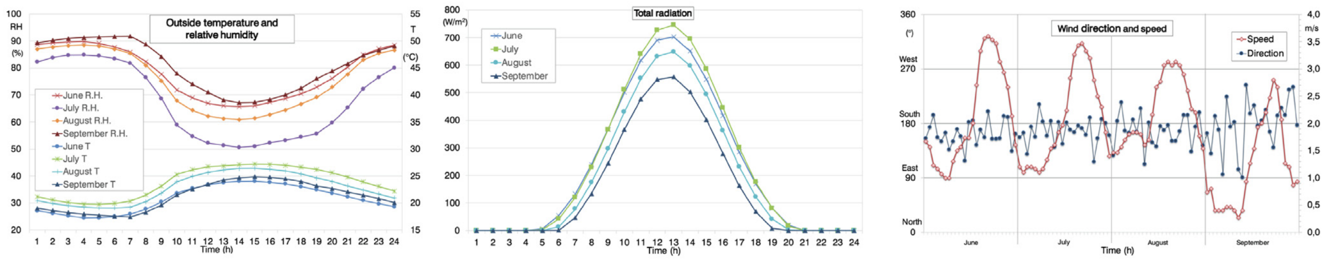

a) b) c)

Fig. 2. Meteorological hourly data of the monthly mean days forced in the ENVI-met simulations.

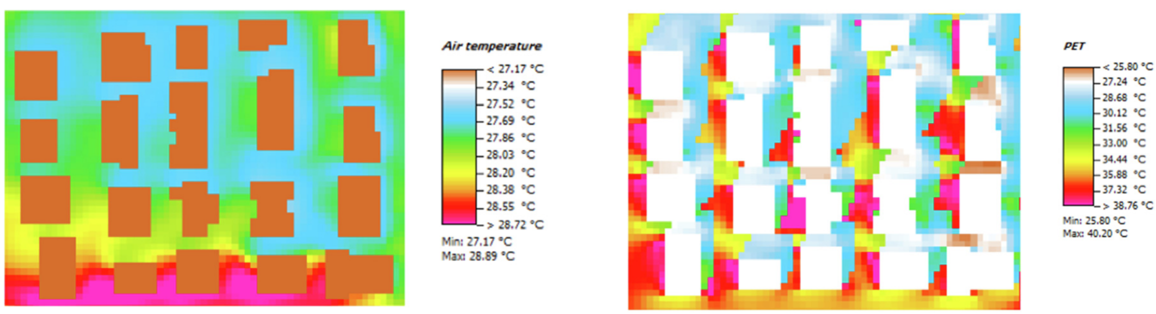

a) b)

Fig. 3. Calculated air temperature map (a) and corresponding PET distribution (b) at height of 1.8 m in August at 1 pm.

ENVI-met, the PET index is calculated based on a simplified form of the Munich Energy Balance Model for Individuals (MEMI) proposed by Höppe [3] and improved by Walther and Goestchel [48]. PET quantifies thermal comfort in terms of temperature with a common unit (°C) and can therefore be easily understood and also used to compare results in different climates [49,50]. Consequently, a human comfort scale based on the PET values was developed to estimate different degrees of human thermal perception and physiological stress in an outdoor environment.

In Table 1, this classification of comfort based on PET is reproduced in the form elaborated by Matzarakis et al. [50] for the Central European climate. The human thermal sensation is classified as cool when the PET value is below 13 °C, and as very hot when the PET value is above 41 °C. The neutral comfort condition for PET is in the range of 18 to 23 °C.

In Fig. 3b shows a visualization of the PET map computed by ENVI-met at an altitude of 1.8 m for the area studied. The remarkable variability of PET in the map highlights the validity of using a value averaged in this area in the analysis, which is more representative than values in individual points. For a more precise comparison of the different mitigation technologies, two indices were introduced to better highlight the advantage over the reference scenario resulting from the application of one solution, both in absolute and relative terms. Eq. (1) calculates the absolute difference DPET (°C) between the PET in the reference scenario (PET_{ref}) and the corresponding final PET obtained:

$$DPET = PET_{ref} - PET \quad (1)$$

Since in the PET scale a temperature value of 23 °C is considered as the limit of neutral comfort sensation, the study was dedicated to the condition where PET is above this value in order to investigate human perception under hot conditions. For this aim, the DPET index was used and calculated only when the average PET of the reference scenario is above 23 °C. This is because, only in this case, human comfort is considered to have to be improved in a summer condition.

DPET expresses the efficacy of the solution in reducing the value of PET, but is not directly related to the improvement of comfort. Therefore, in Eq. (2), the further index %DPET (%) is proposed to represent the effectiveness in terms of comfort benefit:

$$\%DPET = 100 * \frac{DPET}{(PET_{ref} - 23)} \quad (2)$$

The %DPET is the DPET, i.e., the PET reduction after application of a mitigation measure, expressed as a percentage relative to the discomfort quota in the reference scenario. This discomfort quota is quantified as the difference between PET_{ref} and the neutral human sensation threshold in the PET scale, which is 23 °C. It is important to note that these two indices can change in very different ways for the same mitigation intervention.

Table 1
Human perceptions corresponding to PET values.

Thermal sensation	PET range [°C]
Very cold	<4
Cold	4–8
Cool	8–13
Slightly cool	13–18
Neutral	18–23
Slightly warm	23–29
Warm	29–35
Hot	35–41
Very Hot	>41

2.5. Modeling of the mitigation solutions investigated

The main parameters introduced in the model description are listed in Table 2.

Table 2
Properties of the simulated solutions required by ENVI-met.

Cool roof properties (new coating)	SRI	105
	Emissivity (–)	0.9
	Albedo (–)	0.84
Green roof properties (sedum)	LAI (m^2/m^2)	2.0
	Leaf Angle Distribution (–)	0.5
	Plant thickness (cm)	50
	Albedo (–)	0.15
Green wall properties (ivy)	LAI (m^2/m^2)	1.5
	Leaf Angle Distribution (–)	0.5
	Plant thickness (cm)	30
	Albedo (–)	0.2
Greenery substrate properties (sandy loam)	Emissivity (–)	0.9
	Albedo (–)	0.3
	Soil thickness (cm)	15
	Water coefficient (–)	0.5

2.5.1. Cool roof model

The intervention in the original roof consists in a strong increment of the solar reflectance. In the simulation with ENVI-met, the value of 0.42 [51] is assumed for the original reference case with tiles. Then, the same simulations were repeated, introducing for the roof a final value of 0.84 for the solar reflectance. In both cases, the thermal emissivity is assumed to be 0.9, which is a common average value for this type of surfaces. In this way, SRI of the roof from the initial value of 54 reaches a value of 105 after the intervention in the roof [52]. To reach this value of SRI, several actions are possible, such as treating the roof tiles with highly reflective paints or coatings, laying new white tiles or metal tiles characterized by high SRI values.

2.5.2. Greenery models

2.5.2.1. The modeling of vegetation in ENVI-met. ENVI-met simulates the dynamic interaction of the vegetation layer with the surrounding environment and in particular with soil, air, sky and visible urban surfaces. The vegetation is considered as a living organism, where the heat and vapor fluxes must take into account the phenomena of evaporation and transpiration through the leaves, by introducing a sub-model that simulates the opening and closing of the stomata of the leaves. The simulation of new greening modules requires a specific validation of the model through the monitoring of prototypes [53,54]. On the other hand, many studies are not characterized by the introduction of new or local vegetation types, but focus on the impact of a typical greening on different urban forms [55,56]. In this case, the reference to well-known and already validated vegetation modules is frequently used and usually accepted [57,58].

2.5.2.2. Green roof. Given the limited structural capacity of the existing buildings in the area, the retrofit action calls for the use of an extensive green roof with sedum planting. The green roofs will be installed on the roof slopes as a replacement for the roof tiles. For the green roof studied here, a soil thickness of 15 cm and a plant height of 50 cm for the sedum were considered. Another important parameter to consider is the foliage density of the plants, as it plays a fundamental role in the green roof's ability to reduce the air temperature and energy demand of the building. Foliage density is named Leaf Area Density and is defined as the total one-sided leaf area per unit volume [59]. It controls the solar radiation intercepted by the leaves and consequently the temperature of the soil surface [60]. Based on this parameter, the Leaf Area Index LAI is introduced, which is the projection of the total leaf area onto the soil surface [61], i.e., the green leaf area per unit area of the ground surface. In the simulation of the green roof, a value of LAI equal to 2 was assumed, which is typical for sedum [57].

2.5.2.3. Green wall. ENVI-met is equipped with a module to simulate the effects of facade greening on the energy performance of a building and on the urban climate. The properties of the vegetation layer and of the soil layer next to the wall, have to be introduced into the model, if necessary.

The model calculates heat and vapor exchanges within and between the vegetation canopy and the substrate layer by considering plant interactions with the soil and atmosphere. Shortwave and longwave radiation fluxes on the green surface are assessed, as well as radiation reflections with the building walls [62,63]. As for the greening properties, the main input parameters required by the program are LAI, plant thickness, and Leaf Angle Distribution which is evaluated based on the orientation of the leaves and plays an important role in the solar transmission mechanism. For the substrate, the emissivity, albedo, and water content are required. For ivy (Hedera helix), the default values of the program were used. It was assumed that the ivy is planted in several modular, prefabricated boxes that are attached to the vertical surfaces of the building without an air gap. The boxes are filled with sandy loam soil and the ivy is planted in this substrate.

3. Results and discussion

Monitoring of outdoor air temperatures was conducted on a few selected days in the middle of each summer month to test the reliability of the model. Specifically, June 22, July 15, August 18, and September 10 were considered. A sensor (called receptor) to collect the corresponding air temperature calculated by ENVI-met (receptor temperature) was selected at the same location in the area model. Fig. 4 shows the comparison between the hourly trends of this monitored temperature and the corresponding receptor temperature at the same location. Then, the relative coefficient of determination R^2 was calculated for the outdoor air temperature at the receptor point during the four days of summer period. The hourly trends of the contemporary mean air temperature of the area are also reported. The mean air temperature of the area is the average value of air temperatures calculated in all cells of the area at 1.8 m height using ENVI-met. In addition, Fig. 4 shows the coefficients of determination R^2 of the comparison of the monitored temperatures with the calculated temperatures.

The R^2 assessment refers to the whole day or is limited to the daytime hours. In fact, the analysis shows that ENVI-met generally underestimates temperatures at nighttime and evaluates them better during the daytime. In any case, the R^2 (R^2day) referred to the whole day remains in an acceptable range between 0.813 and 0.847 and in agreement with previous studies [57,64]. However, during the central part of the day, i.e., considering the interval from 9 am to 9 pm, the corresponding R^2 (R^2daytime) reaches excellent values, ranging from 0.898 to 0.923. This is particularly significant, because the following analysis focused on this daytime period when the comfort conditions resulted more critical. As for the daily profile of the mean temperature in the area, Fig. 4 shows an excellent agreement with the corresponding profile of the air temperature at the receptor point. In terms of daily averages, the corresponding values are almost identical. Therefore, the experimental validation of the model can be considered significant for the whole simulated area, since the receptor point was placed in a truly representative location. The analysis of discomfort at pedestrian level is based on the average PET relative to all PETs calculated in the cells at a height of 1.8 m in the studied area. The change in this area average PET is used as a criterion for evaluating the effect of the mitigation interventions here analyzed. For this

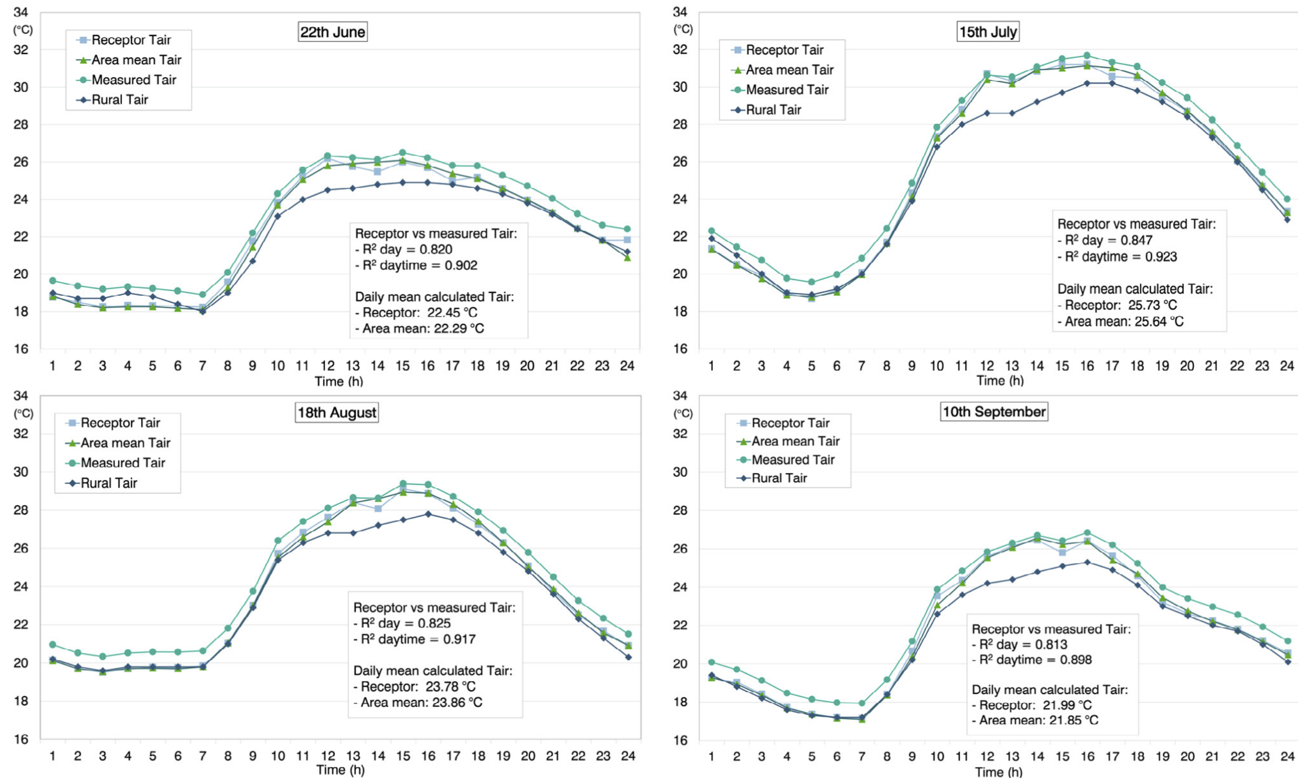

Fig. 4. Daily profiles of the receptor and measured air temperatures at the same location. Calculated area mean air temperatures trends in the same days are also reported.

reason, the first step was to calculate these average PETs for the real condition, i.e., without interventions, of the urban area used as a reference scenario. Then, the average PET values were calculated for the area considering each solution to reduce the overheating effects associated with the urban context. For each scenario, the simulations were performed using ENVI-met on the four monthly mean days. Fig. 5 shows the daily trends of the area average PETs in the reference scenario and after the application of each mitigation technology for the four monthly mean days.

The corresponding DPETs are reported if calculated, i.e., when PET_{ref} is greater than 23 °C. Fig. 5 refers to the case of midrise which is the actual rise of the considered area on the Venice mainland. As for the reference case, PET profiles indicate a clear condition over the neutral limit at pedestrian level during the central daytime on the monthly mean days. It is important to point out that each profile refers to the average weather conditions during the month, and therefore covers the entire monthly period, rather than to the hottest days. The discomfort hourly interval, i.e., the hours when the reference PETs are above 23 °C, is variable in each month. The maximum widths of this interval are in July (9–21) and then in August (10–19). Regarding PETprofiles after the application of mitigation measures, a net benefit of the green wall is evident. The impacts of the mitigation interventions concerning the roofs are more modest and therefore better evaluated when considering the DPETs. For the green roof solution the DPETs result always faintly higher than with cool roof. A slight tendency for the green wall DPET peaks to shift towards the afternoon compared to the cool roof and green roof values is generally observed throughout the season.

Fig. 6 shows the same comparison based on PET and DPET hourly profiles as in the previous Fig. 5, but now refers to the lowrise case. The comparison with the midrise highlights significant differences. As for PET profiles, the comfort at pedestrian level results clearly worsened. This is due to the lower height of the building, as the influence of solar radiation is greater at street level. All PET profiles have grown significantly, especially in August.

Fig. 7 reports the hourly PET and DPET trends for the case of highrise. As concerns a comparison between the reference scenario of the three LCZs, highrise has the lower PET profiles and thus the better initial conditions. Therefore, all the hours are in a PET range lower than the one corresponding to the Hot thermal sensation.

The values of the green walls PET are greatly reduced by increasing the wall heights to which the green walls are attached. For this reason, the trend of PET in this intervention is always below the limit of 23 °C in August and above it only for one hour in June and September.

Fig. 8 shows mean and peak values of the area average DPETs obtained with the mitigation strategies considered for each monthly typical day for the three LCZs. In addition, the corresponding %DPETs are also given. In general, it can be observed that each mitigation solution causes a larger DPET for the peak values than for the average values, since all measures lead to a larger reduction in the hours when the comfort condition is worse. However, the DPETs and %DPETs generally increase at different rates and thus may provide different quantitative indications in the various months. For example, for all the LCZs, mean and peak DPETs are the highest in July while the %DPETs assume the lowest values in that month. In Fig. 8a, the values are referred to midrise. In the case of the green wall, Fig. 8a highlights high mean %DPETs, which range from 38.5 % to 48.7 %, and the higher values for the mean %DPETs than the peak ones. This means that the mitigation effect is effective throughout the day. Different considerations can be made for green and cool roofs. For these measures, the mean %DPETs are lower. In addition, peak %DPETs are now typically higher than average values. Therefore, they appear to perform better during peak hours than during the entire daytime.

In Fig. 8b with the lowrise, there is a clear reduction in DPETs relative to the green wall, which is due to a lower greening area,

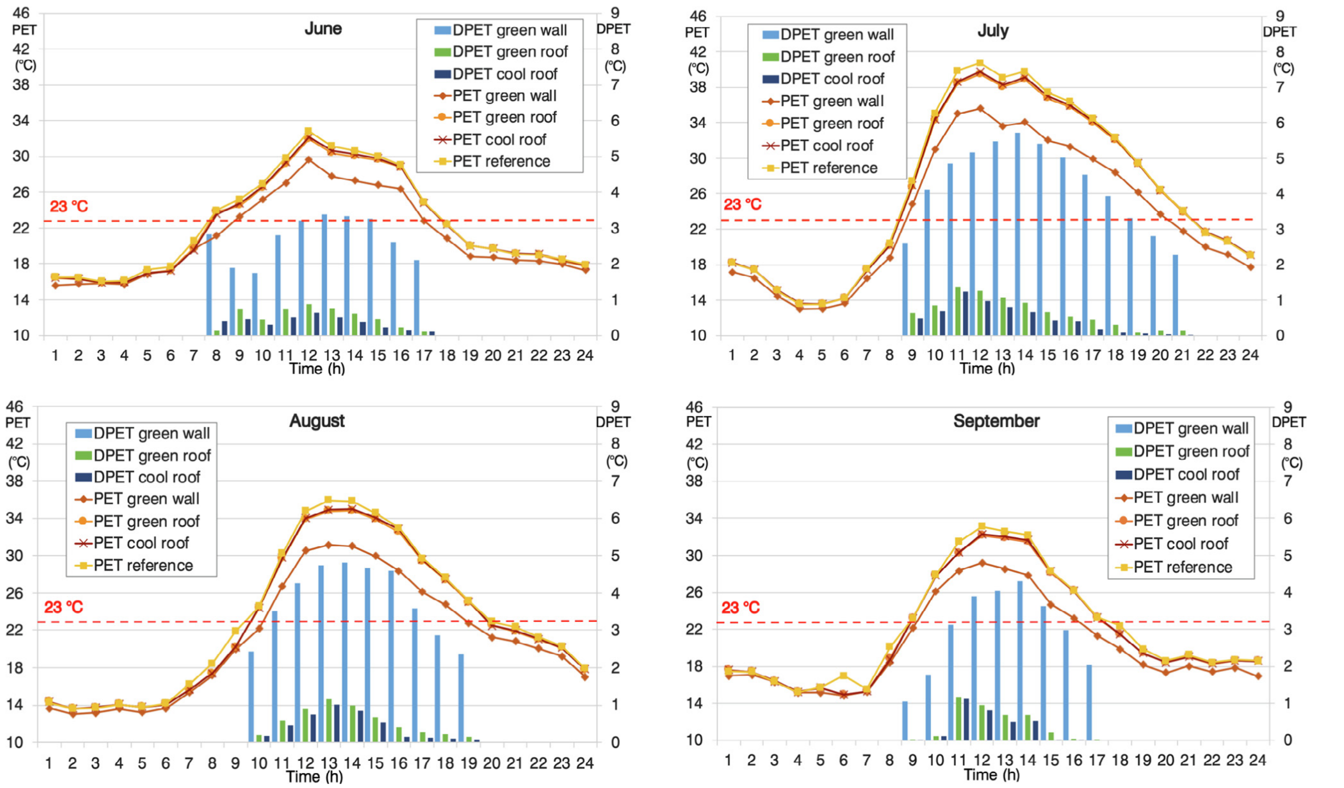

Fig. 5. Area average PET trends for all the studied scenarios and relative DPET trends obtained with the mitigation strategies for each monthly typical day in the case of midrise.

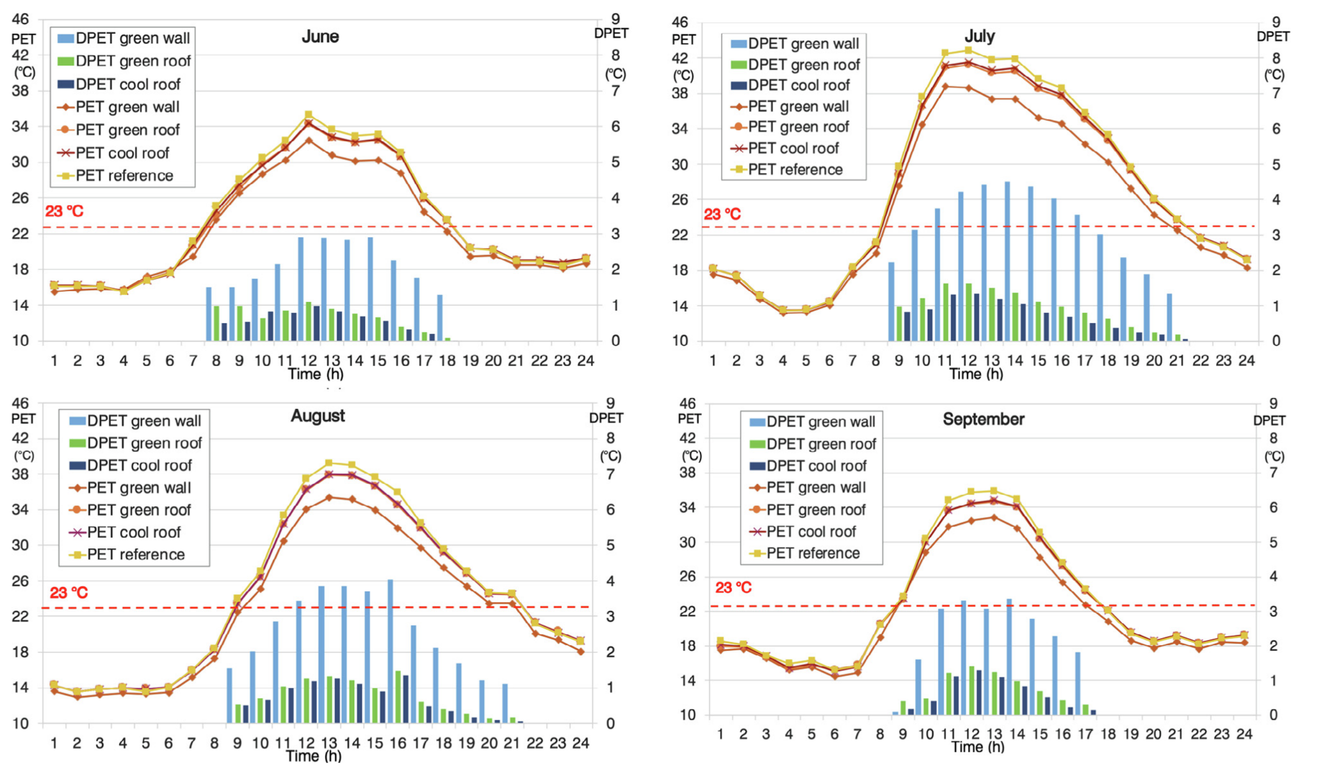

Fig. 6. Area average PET trends for all the studied scenarios and relative DPET trends obtained with the mitigation strategies for each monthly typical day in the case of lowrise.

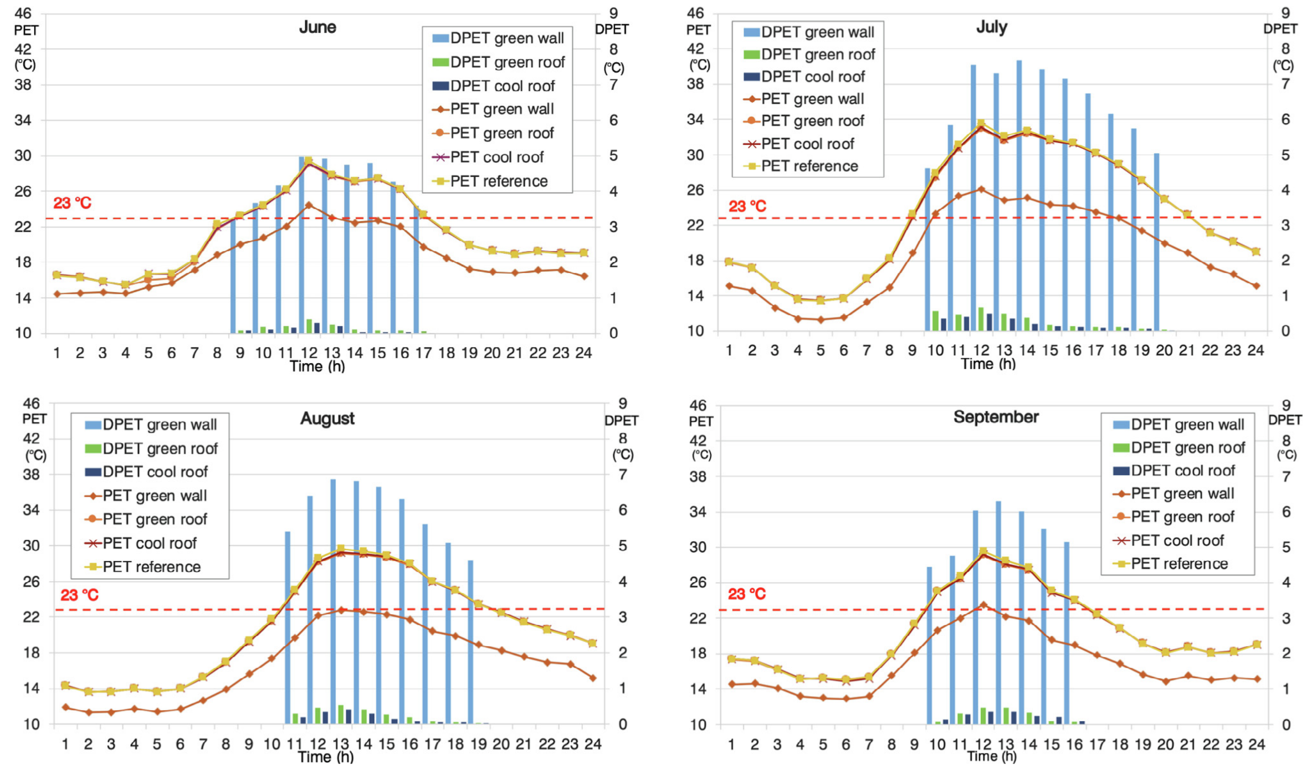

Fig. 7. Area average PET trends for all the studied scenarios and relative DPET trends obtained with the mitigation strategies for each monthly typical day in the case of highrise.

even though they continue to have the highest values. An evident DPET improvement concerns green and cool roofs both in mean and peak values. In terms of %DPETs, for the green wall now the maximum is 30 % in June. For green and cool roofs, the peak values remain higher than the mean ones. However, the increment versus the midrise values is greater for the mean %DPETs rather than for the peak ones. Fig. 8c confirms the excellent performance of the highest vertical greenery in terms of PET reduction with highrise which was already seen in Fig. 7. The lowering of the PET profiles below 23 °C involves %DPETs greater than 100 %. It is interesting to note the important contribution at street level (1.8 m) of the vertical greenery surface quota installed at heights between 20 and 40 m, which is present only in the case of highrise. Only in July, the %DPETs is lower than 100 %, at 90 %. On the contrary, the advantages of green and cool roofs are strongly downscaled.

Fig. 9 reports the frequency distributions as a percentage of the daytime (hours 9–21) of PETs referred to the comfort classification for each scenario and for the three LCZs on the four monthly typical days. In this case, the frequency distribution was calculated considering the PET of each cell of the studied area rather than the averages in the area as in the previous figures. In this way, the behavior in each cell can be examined in detail, considering, for example, the different impacts of building shadows in different zones of the area. The frequency distributions allow to underline more effectively the positive effect to reduce the highest PET values, even in the cases where no extension of the neutral condition is observed for green and cool roofs. Figs. 8 and 9 highlight strong variability in the benefits achieved in the various months for the same intervention and LCZ typology, which is accentuated by the different monthly performance responses of DPETs and %DPETs. No single monthly mean day can be considered representative of the entire summer and a seasonal assessment is necessary. Therefore, a seasonal calculation was made based on the results relative to the monthly mean days. Specifically, the averages from the previously evaluated daily profiles were used to build the corresponding seasonal averages by weighting them by the number of hours in the discomfort interval and days in each month. As mentioned earlier, only 15 days were considered for September. Fig. 10a shows these seasonal values of mean DPETs and %DEPTs. Although aggregating monthly data reduces the peak effectiveness of mitigation strategies found at monthly level analysis, comparison of mitigation strategies at the seasonal level illustrates values/points that are significantly different from monthly analysis. For example, the monthly mean %DPETs range from 90 % to 148 %, while the seasonal mean value is 115 % for the green wall and highrise. Similarly, they range from 7.7 % to 10.5 % and the seasonal value is 9.1 % for green roof and lowrise. For cool roof and lowrise they range from 5.8 % to 8.2 % and the seasonal value is 7.5 %. These numerical differences confirm the opportunity of extending the analysis to the entire summer period to obtain a more correct quantification of the benefits of a mitigation solution.

In the same way, the seasonal frequency distributions of PETs in the comfort ranges were obtained for each scenario considered and presented in Fig. 10b. As in Fig. 9, these frequency distributions are obtained starting from the PETs of the single cells. The seasonal assessment again provides different values than the monthly ones, and thus a temporal distribution of comfort values that is more correct for the whole summer.

4. Contributions of this study

ENVI-met 4.45, used here, includes new procedures for wall and roof greening, to increase the ability to simulate the interactions between vegetation, substrate layer, and attachment materials on facades or roofs [62,63]. These are important improvements for the present study, which focuses on the performance of green walls and roofs. Regarding vegetation, a review paper [31] highlighted the limited studies on the effects of vertical greening on

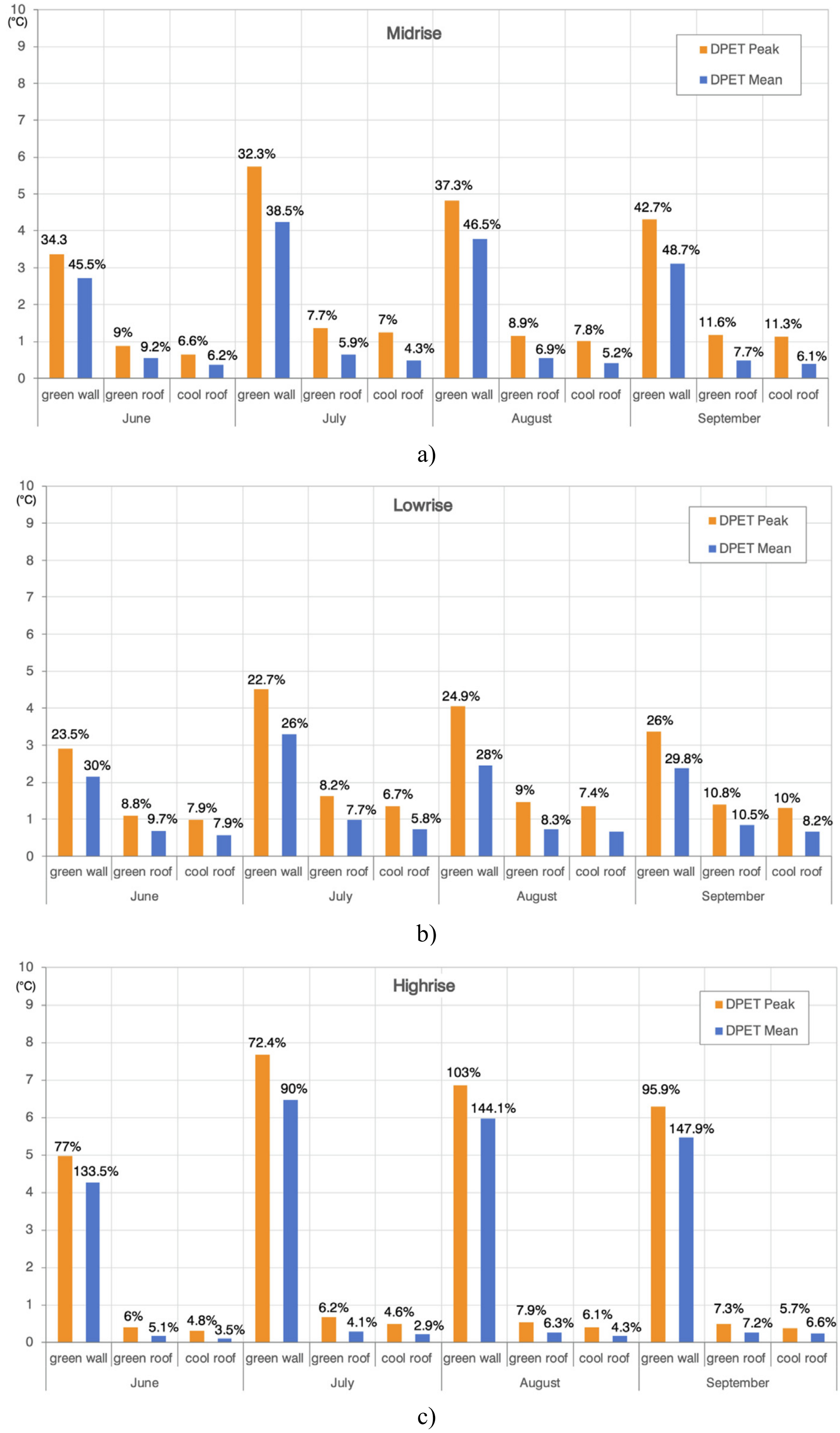

Fig. 8. Mean and peak DPET trends with mitigation strategies for each monthly typical day in the three LCZs. The corresponding %DPETs are also indicated above the bars.

the PET index, which is due to the recent introduction of more accurate greening modeling in the ENVI-met software. Continued development of ENVI-met is stimulating new applications of vegetation modeling [65]. This is the case with this study, which focuses on the impact of installing green infrastructure in buildings. Important confirmations of the effectiveness of greening were found, particularly in hot [35] and continental [66] climates and in high-density cities such as Hong Kong [64] and Cairo [67]. In this study, an evaluation of the benefits for the northern Mediterranean climate and considering LCZs typical of European urban areas was carried out. The approach adopted has three innovative aspects. First, the monthly assessment. Indeed, several studies have focused

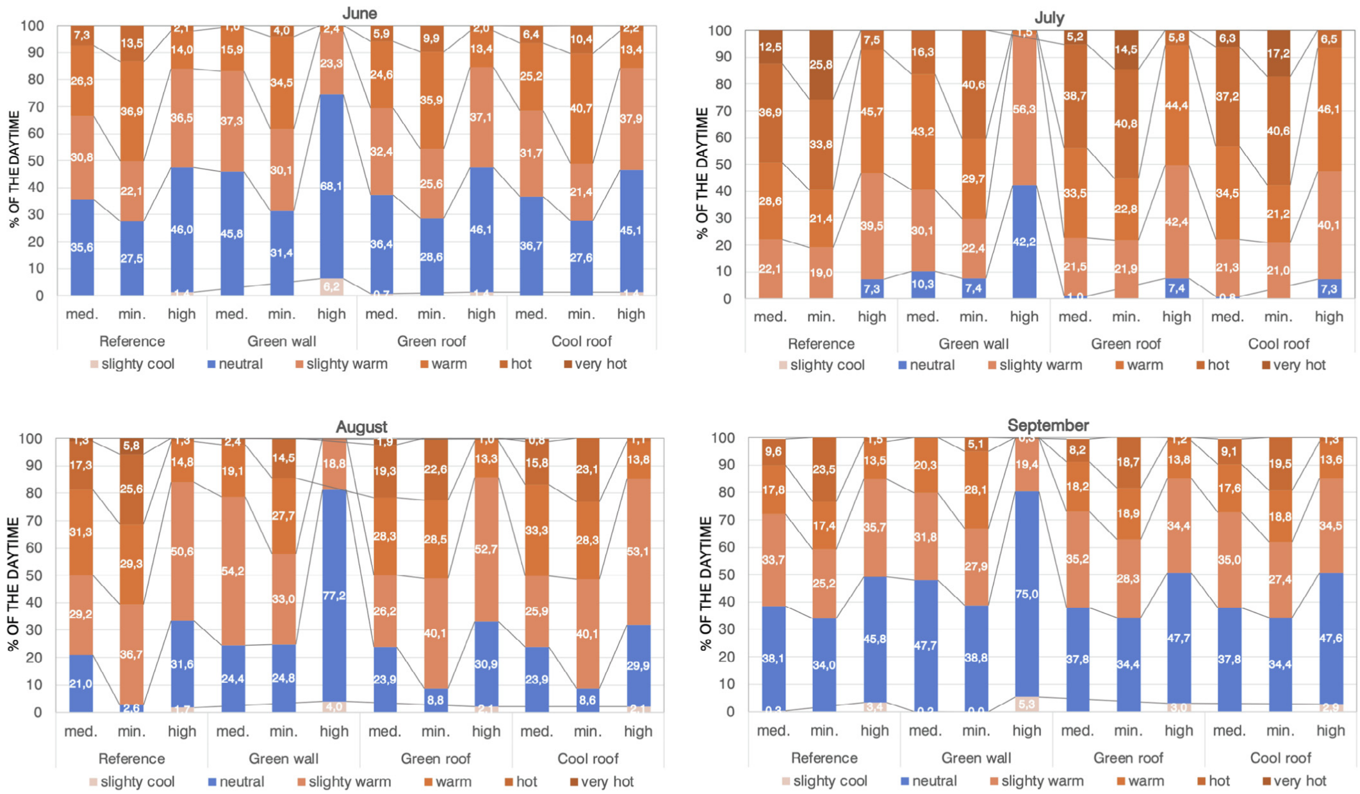

Fig. 9. Frequency distribution (%) of the area mean PETs refers to the comfort classes for each scenario and for the three LCZs in the four monthly typical days.

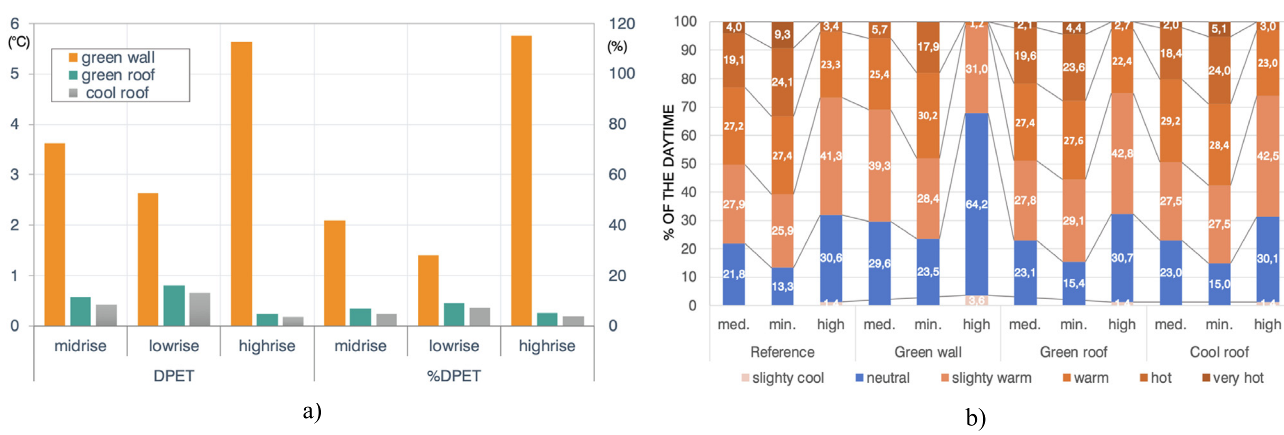

Fig. 10. Average summer values of DPETs and %DPETs a) and of the frequency distribution (%) b) for each scenario and the three LCZs.

on the outdoor thermal comfort at the microscale level [68–71]. However, due to the high computational time, ENVI-met is usually used to simulate single days [72]. Consequently, the studies are conducted on a few days, usually selected about the hottest days of summer, to highlight the effects of mitigation measures under the worst conditions rather than over a long period of time. In this work, monthly mean days obtained from real meteorological data were used instead of a few real days in the period. An analysis based on monthly mean days allows the extension of validity to the entire summer and overcomes the limitations of difficult generalization resulting from simulating individual summer days. In this way, the results are more representative, as climatic conditions strongly influence the impact of mitigation strategies. Considering that the goal is to improve human comfort along an extended period, the use of average weather conditions is opportune. Second, the analysis was performed using an average PET value of the studied area, obtained from the corresponding values of all cells of the corresponding ENVI-met model for each simulated scenario. This procedure was validated by evaluating the PET frequency distributions from each cell of the studied area, which gave matching results. Third, the introduction of the %DPET index. In the previous studies [31,32], the change in the index PET is directly used as a comparative tool to evaluate the improvement compared to the urban reference scenario. In this study, a new algorithm based on PET is proposed for this purpose to better evaluate the benefit in terms of comfort threshold. The %DPET index expresses the effectiveness in terms of relative comfort benefit, i.e., in relation to the discomfort gap of the corresponding reference scenario. It complements the DPET index, which quantifies the ability of each technology to reduce the value of PET in absolute terms. The different results obtained by using DPET or %DPET demonstrate the advantage of using the two indices in combination. The averaged values of these indices facilitate the extension of the analysis to monthly and seasonal time periods.

5. Conclusion

Different results were obtained in different monthly weather conditions underlining the fundamental importance of climate in the evaluations. Therefore, an assessment based on monthly mean days confirmed its better suitability to examine the mitigation effects on a seasonal level. In addition to the DPET index, the % DPET, which directly relates to the reduction in the discomfort gap of the individual reference scenario, allows for a more comprehensive assessment of the effectiveness of each mitigation strategy. In fact, in the same case studied, the simulation provided different trends in terms of DPETs or %DPETs. As for the thermal mitigation at 1.8 m quota, the interventions at roof level are resulted very sensitive to the height of the buildings and useful, especially in the case of LCZ 3 Compact lowrise. Here, the simpler and cheaper cool roof technology has provided an average summer %DPET of 7.5 %, which is not much lower than that of the green roof (9.1 %). However, the choice should also consider the other benefits of the green roof, such as stormwater capture and air quality improvement. To improve pedestrian comfort, the best technology for the building envelope is resulted the introduction of vertical greenery. In all three compact LCZs analyzed here, the advantage over the other solutions is clearly highlighted and increases sharply with building height, with average summer %DPET ranging from 28 % to 115 %. Thus, in the highrise buildings, the vertical greenery systems allowed to move PET into the comfort zone for almost all the simulated periods.

CRediT authorship contribution statement

Luigi Schibuola: Conceptualization, Methodology, Writing – original draft, Supervision. **Chiara Tambani:** Data curation, Methodology, Software, Investigation, Writing – original draft, Writing – review & editing.

Data availability

Data will be made available on request.

Declaration of Competing Interest

The authors declare that they have no known competing financial interests or personal relationships that could have appeared to influence the work reported in this paper.

References

[1] M.E. Gonzalez-Trevizo, K.E. Martinez-Torres, J.F. Armendariz-Lopez, M. Santamouris, G. Bojorquez-Morales, A. Luna-Leon, Research trends on environmental, energy and vulnerability impacts of Urban Heat Islands: An overview, Energy Build. 246 (2021), https://doi.org/10.1016/j.enbuild.2021.111051 111051.
[2] L. Schibuola, C. Tambani, Performance assessment of seawater cooled chillers to mitigate urban heat island, Appl. Therm. Eng. 175 (2020), https://doi.org/10.1016/j.applthermaleng.2020.115390 115390.
[3] P. Höppe, The physiological equivalent temperature - A universal index for the biometeorological assessment of the thermal environment, Int. J. Biometeorol. 43 (2) (1999) 71–75.
[4] R. de Dear, J. Kalma, T. Oke, An outdoor thermal comfort index (Out_SET*)–Part 1–The model and its assumptions. In book: Biometeorology and Urban Climatology at the Turn of the Millennium. WCASP 50: WMO/TD No.1026, Geneva Edi, (2020).
[5] G. Jendritzky, R. de Dear, G. Havenith, UTCI-Why another thermal index?, Int J. Biometeorol. 56 (3) (2012) 421–428.
[6] O. Potchter, P. Cohen, T.-P. Lin, A. Matzarakis, Outdoor human thermal perception in various climates: A comprehensive review of approaches, methods and quantification, Sci. Total Environ. 631-632 (2018) 390–406.
[7] Y. Wang, Z. Ni, S. Chen, B. Xia, Microclimate regulation and energy saving potential from different urban green infrastructures in a subtropical city, J. Clean. Prod. 226 (2019) 913–927, https://doi.org/10.1016/j.jclepro.2019.04.114.
[8] F. Bisegna, A. Buggin, G. Peri, G. Rizzo, G. Scaccianoce, M. Scarpa, L. Schibuola, C. Tambani, Computing methods for resilience: Evaluating new building components in the frame of SECAPs, in: Proc. - 2019 IEEE Int. Conf. Environ. Electr. Eng. 2019 IEEE Ind. Commer. Power Syst. Eur. EEEIC/I CPS Eur. (2019). https://doi.org/10.1109/EEEIC.2019.8783458.
[9] D.D. Lorenzo, B.M.L. Casto, G. Peri, G. Rizzo, G. Scaccianoce, C. Tambani, Enhancing values of roofs albedo for lowering cities' air temperature and electric demand of buildings: a simple economic evaluation, IOP Conf. Ser.: Mater. Sci. Eng. 609 (7) (2019) 072049.
[10] M. Taleghani, U. Berardi, The effect of pavement characteristics on pedestrians' thermal comfort in Toronto, Urban Clim. 24 (2018) 449–459.
[11] A. Aboelata, Reducing outdoor air temperature, improving thermal comfort, and saving buildings' cooling energy demand in arid cities – Cool paving utilization, Sustain. Cities Soc. 68 (2021) 102762.
[12] A. Synnefa, M. Santamouris, I. Livada, A study of the thermal performance of reflective coatings for the urban environment, Sol. Energy. 80 (8) (2006) 968–981.
[13] A. Synnefa, M. Santamouris, K. Apostolakis, On the development, optical properties and thermal performance of cool colored coatings for the urban environment, Sol. Energy. 81 (2007) 488–497, https://doi.org/10.1016/j.solener.2006.08.005.
[14] A. International, ASTM E1980-11—Standard Practice for Calculating Solar Reflectance Index of Horizontal, (2019).
[15] U.S. Green Building Council, LEED v4 CREDITS for Building Design and Construction, LEED Publ. (2019).
[16] G. Peri, G. Rizzo, G. Scaccianoce, M. La Gennusa, P. Jones, Vegetation and soil – related parameters for computing solar radiation exchanges within green roofs: Are the available values adequate for an easy modeling of their thermal behavior?, Energy Build 129 (2016) 535–548.
[17] C.M. Silva, M.G. Gomes, M. Silva, Green roofs energy performance in Mediterranean climate, Energy Build. 116 (2016) 318–325.
[18] C.Y. Jim, S.W. Tsang, Biophysical properties and thermal performance of an intensive green roof, Build. Environ. 46 (6) (2011) 1263–1274.
[19] B.-S. Lin, C.-C. Yu, A.-T. Su, Y.-J. Lin, Impact of climatic conditions on the thermal effectiveness of an extensive green roof, Build. Environ. 67 (2013) 26–33.
[20] M. Mahmoodzadeh, P. Mukhopadhyaya, C. Valeo, Effects of extensive green roofs on energy performance of school buildings in Four North American climates, Water (Switzerland) 12 (1) (2020) 6.
[21] US EPA, Reducing Urban Heat Islands: Compendium of Strategies | Heat Island Effect | US EPA, Us Epa. (2013).
[22] K. Vijayaraghavan, Green roofs: A critical review on the role of components, benefits, limitations and trends, Renew. Sustain. Energy Rev. 57 (2016) 740–752.
[23] S.A. Palermo, M. Turco, Green Wall systems: Where do we stand?, IOP Conf Ser. Earth Environ. Sci. 410 (1) (2020) 012013.
[24] K. Perini, M. Ottelé, E.M. Haas, R. Raiteri, Vertical greening systems, a process tree for green façades and living walls, Urban Ecosyst. 16 (2) (2013) 265–277.
[25] I.D. Stewart, T.R. Oke, Local climate zones for urban temperature studies, Bull. Am. Meteorol. Soc. 93 (12) (2012) 1879–1900.
[26] I.D. Stewart, T.R. Oke, E.S. Krayenhoff, Evaluation of the 'local climate zone' scheme using temperature observations and model simulations, Int. J. Climatol. 34 (4) (2014) 1062–1080.
[27] A. Rodler, T. Leduc, Local climate zone approach on local and micro scales: Dividing the urban open space, Urban Clim. 28 (2019) 100457.
[28] B. Bechtel, P. Alexander, J. Böhner, J. Ching, O. Conrad, J. Feddema, G. Mills, L. See, I. Stewart, Mapping local climate zones for a worldwide database of the form and function of cities, ISPRS Int. J. Geo-Information. 4 (1) (2015) 199–219.
[29] M. Demuzere, S. Hankey, G. Mills, W. Zhang, T. Lu, B. Bechtel, Combining expert and crowd-sourced training data to map urban form and functions for the continental US, Sci. Data 7 (1) (2020), https://doi.org/10.1038/s41597-020-00605-z.
[30] M. Bruse, H. Fleer, Simulating surface-plant-air interactions inside urban environments with a three dimensional numerical model, Environ. Model. Softw. 13 (3-4) (1998) 373–384.
[31] C.K.C. Lam, H. Lee, S.-R. Yang, S. Park, A review on the significance and perspective of the numerical simulations of outdoor thermal environment, Sustain. Cities Soc. 71 (2021), https://doi.org/10.1016/j.scs.2021.102971 102971.
[32] S. Tsoka, A. Tsikaloudaki, T. Theodosiou, Analyzing the ENVI-met microclimate model's performance and assessing cool materials and urban vegetation applications–A review, Sustain. Cities Soc. 43 (2018) 55–76, https://doi.org/10.1016/j.scs.2018.08.009.
[33] H. Mayer, J. Holst, P. Dostal, F. Imbery, D. Schindler, Human thermal comfort in summer within an urban street canyon in Central Europe, Meteorol. Zeitschrift 17 (3) (2008) 241–250.
[34] T.E. Morakinyo, Y.F. Lam, Simulation study on the impact of tree-configuration, planting pattern and wind condition on street-canyon's micro-climate and thermal comfort, Build. Environ. 103 (2016) 262–275.

[35] W. Ouyang, T. Sinsel, H. Simon, T.E. Morakinyo, H. Liu, E. Ng, Evaluating the thermal-radiative performance of ENVI-met model for green infrastructure typologies: Experience from a subtropical climate, Build. Environ. 207 (2022), https://doi.org/10.1016/j.buildenv.2021.108427 108427.
[36] T.E. Morakinyo, K.-L. Lau, C. Ren, E. Ng, Performance of Hong Kong's common trees species for outdoor temperature regulation, thermal comfort and energy saving, Build. Environ. 137 (2018) 157–170.
[37] U.S. Department of Energy, EnergyPlus Version 9.2.0, Documentation-Auxiliary Programs. (2019). https://energyplus.net/sites/all/modules/custom/nrel_custom/pdfs/pdfs_v9.2.0/AuxiliaryPrograms.pdf.
[38] X. Yang, L. Zhao, M. Bruse, Q. Meng, Evaluation of a microclimate model for predicting the thermal behavior of different ground surfaces, Build. Environ. 60 (2013) 93–104.
[39] A. Middel, K. Häb, A.J. Brazel, C.A. Martin, S. Guhathakurta, Impact of urban form and design on mid-afternoon microclimate in Phoenix Local Climate Zones, Landsc. Urban Plan. 122 (2014) 16–28.
[40] M. Taleghani, M. Tenpierik, A. van den Dobbelsteen, D.J. Sailor, Heat in courtyards: A validated and calibrated parametric study of heat mitigation strategies for urban courtyards in the Netherlands, Sol. Energy. 103 (2014) 108–124.
[41] M.H.E. Mahgoub, N. Hamza, S. Dudek, Microclimatic Investigation of Two Different Urban Forms in Cairo, Egypt: Meassurements and Model Simulations, Build. Simul. Cairo 2013 - Towar. Sustain. Green Built Environ. Cairo. (2013).
[42] J. Ren, J. Yang, Y. Zhang, X. Xiao, J.C. Xia, X. Li, S. Wang, Exploring thermal comfort of urban buildings based on local climate zones, J. Clean. Prod. 340 (2022), https://doi.org/10.1016/j.jclepro.2022.130744 130744.
[43] N. Müller, W. Kuttler, A.-B. Barlag, Counteracting urban climate change: Adaptation measures and their effect on thermal comfort, Theor. Appl. Climatol. 115 (1-2) (2014) 243–257.
[44] L. Peng, C. Jim, Green-roof effects on neighborhood microclimate and human thermal sensation, Energies 6 (2) (2013) 598–618.
[45] L.P. Muniz-Gäal, C.C. Pezzuto, M.F.H.d. Carvalho, L.T.M. Mota, Urban geometry and the microclimate of street canyons in tropical climate, Build. Environ. 169 (2020) 106547.
[46] H. Taha, D. Sailor, H. Akbari, High-Albedo Materials for Reducing Building Cooling Energy Use, Lawrence Berkeley Laboratory, University of California, (1992).
[47] UNI standard, UNI/TR 11552:2014, Abaco delle strutture costituenti l'involucro opaco degli edifici - Parametri termofisici. (2014).
[48] E. Walther, Q. Goestchel, The P.E.T. comfort index: Questioning the model, Build. Environ. 137 (2018) 1–10.
[49] J.-Y. Deng, N.H. Wong, Impact of urban canyon geometries on outdoor thermal comfort in central business districts, Sustain. Cities Soc. 53 (2020) 101966.
[50] A. Matzarakis, H. Mayer, M.G. Iziomon, Applications of a universal thermal index: Physiological equivalent temperature, Int. J. Biometeorol. 43 (2) (1999) 76–84.
[51] A. Muscio, A. Libbra, C. Siligardi, Development of materials with high solar reflection for the optimization of the Energy performance of buildings during the summer season, (2011).
[52] U.S. Environmental Protection Agency., Cool Roofs. In: Reducing Urban Heat Islands: Compendium of Strategies., (2008).
[53] J.A. Acero, K. Herranz-Pascual, A comparison of thermal comfort conditions in four urban spaces by means of measurements and modelling techniques, Build. Environ. 93 (2015) 245–257.
[54] H. Simon, J. Lindén, D. Hoffmann, P. Braun, M. Bruse, J. Esper, Modeling transpiration and leaf temperature of urban trees – A case study evaluating the microclimate model ENVI-met against measurement data, Landsc. Urban Plan. 174 (2018) 33–40.
[55] H. Farhadi, M. Faizi, H. Sanaieian, Mitigating the urban heat island in a residential area in Tehran: Investigating the role of vegetation, materials, and orientation of buildings, Sustain. Cities Soc. 46 (2019) 101448.
[56] T.E. Morakinyo, K.W.D. Kalani, C. Dahanayake, E. Ng, C.L. Chow, Temperature and cooling demand reduction by green-roof types in different climates and urban densities: A co-simulation parametric study, Energy Build. (2017), https://doi.org/10.1016/j.enbuild.2017.03.066.
[57] U. Berardi, The outdoor microclimate benefits and energy saving resulting from green roofs retrofits, Energy Build. 121 (2016) 217–229.
[58] K. Ornam, S. Triyadi, S. Wonorahardjo, I.M. Sutjahja, P. Martonohadi, S. Assegaf, M. Kimsan, Thermal Environment Control of Buildings using Installation of Plants and Metal Panels on Brick Walls, IOP Conf. Ser. Earth Environ. Sci. 738 (1) (2021) 012001.
[59] I. Jonckheere, S. Fleck, K. Nackaerts, B. Muys, P. Coppin, M. Weiss, F. Baret, Review of methods for in situ leaf area index determination, Agric. For. Meteorol. 121 (1-2) (2004) 19–35.
[60] M. Béland, D.D. Baldocchi, J.-L. Widlowski, R.A. Fournier, M.M. Verstraete, On seeing the wood from the leaves and the role of voxel size in determining leaf area distribution of forests with terrestrial LiDAR, Agric. For. Meteorol. 184 (2014) 82–97.
[61] S.S. Alcazar, F. Olivieri, J. Neila, Green roofs: Experimental and analytical study of its potential for urban microclimate regulation in Mediterranean–continental climates, Urban Clim. 17 (2016) 304–317.
[62] M.Bruse, ENVI-met - Decode urban nature with ENVI-met software. Retrieved January 21, 2020, from https: www.envi-met.com, (2019).
[63] H. Simon, Modeling urban microclimate: development, implementation and evaluation of new and improved calculation methods for the urban microclimate model ENVI-met, (2016).
[64] T.E. Morakinyo, A. Lai, K.-L. Lau, E. Ng, Thermal benefits of vertical greening in a high-density city: Case study of Hong Kong, Urban For. Urban Green. 37 (2019) 42–55.
[65] Z. Liu, W. Cheng, C.Y. Jim, T.E. Morakinyo, Y. Shi, E. Ng, Heat mitigation benefits of urban green and blue infrastructures: A systematic review of modeling techniques, validation and scenario simulation in ENVI-met V4, Build. Environ. 200 (2021), https://doi.org/10.1016/j.buildenv.2021.107939 107939.
[66] U. Berardi, Z. Jandaghian, J. Graham, Effects of greenery enhancements for the resilience to heat waves: A comparison of analysis performed through mesoscale (WRF) and microscale (Envi-met) modeling, Sci. Total Environ. 747 (2020), https://doi.org/10.1016/j.scitotenv.2020.141300 141300.
[67] A. Aboelata, S. Sodoudi, Evaluating urban vegetation scenarios to mitigate urban heat island and reduce buildings' energy in dense built-up areas in Cairo, Build. Environ. 166 (2019), https://doi.org/10.1016/j.buildenv.2019.106407 106407.
[68] D. Antoniadis, N. Katsoulas, C. Kittas, Simulation of schoolyard's microclimate and human thermal comfort under Mediterranean climate conditions: effects of trees and green structures, Int. J. Biometeorol. 62 (2018) 2025–2036. https://eurekamag.com/research/065/917/065917588.php.
[69] H. Lee, H. Mayer, Thermal comfort of pedestrians in an urban street canyon is affected by increasing albedo of building walls, Int. J. Biometeorol. 62 (2018) 1199–1209, https://doi.org/10.1007/s00484-018-1523-5.
[70] A. Chatzidimitriou, K. Axarli, Street Canyon Geometry Effects on Microclimate and Comfort; A Case Study in Thessaloniki, Procedia, Environ. Sci. 38 (2017) 643–650, https://doi.org/10.1016/j.proenv.2017.03.144.
[71] S. Yin, W. Lang, Y. Xiao, Z. Xu, Correlative Impact of Shading Strategies and Configurations Design on Pedestrian-Level Thermal Comfort in Traditional Shophouse Neighbourhoods, Southern China, Sustainability 11 (5) (2019) 1355.
[72] D. Lai, W. Liu, T. Gan, K. Liu, Q. Chen, A review of mitigating strategies to improve the thermal environment and thermal comfort in urban outdoor spaces, Sci. Total Environ. 661 (2019) 337–353.